

*Original Research Article***Ponding time, hydraulic conductivity, and sorptivity – experimental and numerical determination**Jana Kalibová¹, Jan Petrů¹, Melorio Luca², Jakub Štibinger¹¹Department of Land Use and Improvement, Faculty of Environmental Sciences, Czech University of Life Sciences Prague, Czech Republic²University of Naples Federico II, Corso Umberto I 40, 801 38 Naples, Italy, lukeblues93@gmail.com**Correspondence to:****J. Štibinger**, Department of Land Use and Improvement, Faculty of Environmental Sciences, Czech University of Life Sciences Prague, Kamýčká 129, Praha – Suchbátka, 165 00, Czech Republic, e-mail: stibinger@fzp.czu.cz**Abstract**

Determination of actual soil sorptivity becomes one of the research preferences in the field of soil management and flash-flood protection. This Note presents an innovative approach to soil sorptivity determination. A single ring infiltration method, along with a simulation of rainfall of constant intensity, was used to measure ponding time t_p . Hydraulic conductivity K was approximated from the analysis of the time series of the process of vertical non-steady cumulative infiltration appearing after the ponding time. Based on Philip's infiltration theory, a simple equation was derived in order to calculate sorptivity S from ponding time, rainfall intensity, and saturated hydraulic conductivity. Numerically determined results of S show to closely correspond with theoretical values published in the literature. To the best of our knowledge, this process of numerical determination of K and S has not been published so far. Moreover, unlike the traditional methods, e.g. single or double-ring in infiltration experiments, this method provides more precise and representative values of S , verified by ponding time, as the results refer to the original soil sorptivity, not the sorptivity determined after the ponding time (meaning sorptivity of the fully saturated environment) which tends to reach zero. Our assumption was definitely confirmed by field experimental determination of ponding time and selected soil hydrology characteristics.

Keywords: infiltration; rainfall simulation; single ring infiltrometer; soil hydraulic properties; rainfall intensity; flash floods

INTRODUCTION

Flood hazards and vulnerability to floods tend to increase over many areas, due to adverse changes in climatic, terrestrial, hydrological, and socio-economic systems (Whitehead et al., 2009; Dirmeyer et al., 2012). Therefore, increasing attention is being paid to upgrading flood protection systems (Alfieri et al., 2012; Borga et al., 2011; Menzel and Kundzewicz, 2003). A flood recast-warning system can provide us with valuable time to either apply specific flood control measures or to evacuate. Current flood forecast-warning systems are generally based on the

threshold runoff estimates used in conjunction with soil moisture accounting models and areal rainfall data (Polger, 1994; Carpenter et al., 1999; Georgakakos, 2006; Javelle et al., 2010; Hapuarachchi et al., 2011). Soil moisture was reported to be a crucial input parameter (Fuentes et al., 2009; Mirlas, 2009; Ntelekos et al., 2006; Norbiato et al., 2008; Singh, 2009).

Soil moisture is closely related to soil sorptivity (Mirlas, 2009; Singh, 2009). Generally, the lower the soil moisture content, the higher the sorptivity (Zhang, 1997; Villarreal et al., 2019). Soil sorptivity and hydraulic conductivity are crucial soil properties

© AUTHORS 2023.

This work is licensed under the Creative Commons Attribution-NonCommercial-NoDerivs 4.0 License (<https://creativecommons.org/licenses/by-nc-nd/4.0/>)

determining the character of rainfall-runoff processes and the risk of surface runoff formation. Usually, soil sorptivity is determined either from laboratory experiments or from cumulative infiltration curves (Angulo-Jaramillo et al., 2000). Both methods are time-consuming and lead to low values of sorptivity as they are derived from saturated soil conditions.

In agreement with the goal of the grant TH02010802 ‘The system of a timely prediction of flash floods based on the direct measurement of infiltration’, an innovative method was developed to predict flash flood risk, using a prototype of a single ring continuous infiltrometer. The flood risk prediction is based on a comparison of design rainfall characteristics and actual soil moisture conditions (ponding time t_p). The flood forecast-warning system itself will be described in more detail in another publication. In this paper, the authors introduce a new approach to the determination of the original soil sorptivity – sorptivity referring to the soil moisture condition before any rainfall is applied onto the soil. Based on Philip’s infiltration theory, a simple equation was derived in order to calculate sorptivity S from ponding time t_p and saturated hydraulic conductivity K . Numerical determination of K and S using this process has not been published so far. Furthermore, unlike the traditional methods, this method is less time-consuming and provides more precise and representative values of S , verified by ponding time. Based on the soil moisture evaluation described in this article, the current flood forecast-warning system comes from the theoretical calculation of ponding time as described here.

MATERIAL AND METHODS

Theory

Theoretical base of the research project comes from non-steady state unsaturated vertical infiltration. This process, in one-dimensional flow conditions (z, t), can be described by Richard’s equation (Eq. 1) (Kutílek and Nielsen, 1994):

$$\frac{\partial v}{\partial z} = \frac{\partial \theta}{\partial t} \tag{1}$$

where: θ – soil moisture [-], v – intensity of infiltration [L/T], z – vertical coordinate [L], t – time [T]. The final simplified solution of Equation 1 is provided by Philip’s simplified infiltration equations (Eq.2, 3) (Phillip, 1957a; Phillip, 1957b).

$$i(t) = S \cdot t^{\frac{1}{2}} + K \cdot t \tag{2}$$

$$v(t) = \left(\frac{1}{2}\right) \cdot S \cdot t^{-\frac{1}{2}} + K \tag{3}$$

Equations 4 and 5 are valid:

$$v(t) = \frac{\partial i(t)}{\partial t} \tag{4}$$

$$i(t) = \int v(t) dt \tag{5}$$

where $i(t)$ – cumulative amount of infiltrated water [L]; $v(t)$ – intensity of infiltration [L/T]; S – sorptivity [L/T^{-1/2}]; K (L/T) – hydraulic conductivity representing the coefficient of long-term infiltration A [L/T]. Symbols L and T represent units of length and time, respectively.

The first term of Equation (Eq. 2) describes the uptake of water by porous media via capillary forces and dominates infiltration when time is short (Phillip, 1957ab). This term contains a coefficient S , which bears a resemblance to the words “permeability,” “capillary conductivity,” and “absorptivity”. The term “sorptivity” is presented by Philip (1957b). Sorptivity embraces both the concepts of absorption and desorption (the ability of the soil pores to absorb and release water by capillarity). Sorptivity may also be discussed in terms of pore-liquid geometry (Phillip 1957b). Although the sorptivity parameter is not a directly measurable soil attribute, it may be derived from actual soil properties (Hanks and Ashcroft, 1976).

It is apparent from Equation (3), that as time proceeds the second term K , which describes the ability of the soil to transmit water due to gravity forces plays an increasingly important role as a driving force (as t approaches infinity, the first term approaches zero, and i approaches K asymptotically).

Phillip (1957a) pointed out that S coefficient varies with initial soil moisture content θ (Jaynes and Gifford, 1981). Then, θ increases during the infiltration process, the sorptivity S decreases, so does the intensity of infiltration v , while the amount of infiltrated water i increases, as shown on the graphs below (Fig. 1, 2).

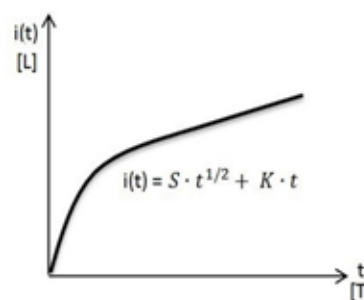


Figure 1. Cumulative infiltration curve

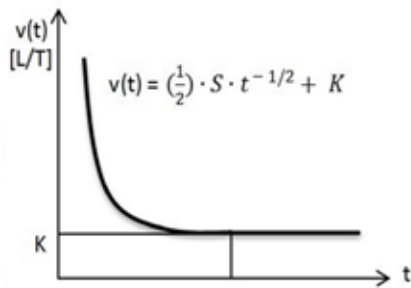


Figure 2. Infiltration rate curve; t_p = ponding time

These curves (Fig. 1, 2) are composed of the first exponential part and the final linear part. It means that when the soil is fully saturated ($S = 0, t \geq t_p$) the following expressions are valid (Eq. 6, 7):

$$i(t) = K \cdot t, \text{ where } t \geq t_p \tag{6}$$

$$v(t) = K, \text{ where } t \geq t_p \tag{7}$$

where t_p is called *ponding time*. t_p represents the time when soil is fully saturated, and it divides the infiltration event into two different periods: the first period is governed by the Neuman Boundary Condition ($i = S \cdot t^{1/2} + Kt; z = 0; 0 < t < t_p$) (NBC) while the second by the Dirichlet Boundary Condition ($i = Kt; z = 0; t \geq t_p$) (DBC). A constant rain intensity $v(t) < K$ produces an infiltration phenomenon governed by NBC, where the term t_p does not appear (Kutílek and Nielsen, 1994).

In order to obtain t_p , it can be considered a constant rainfall intensity $v_r > K$ [mm/min] (Fig. 3):

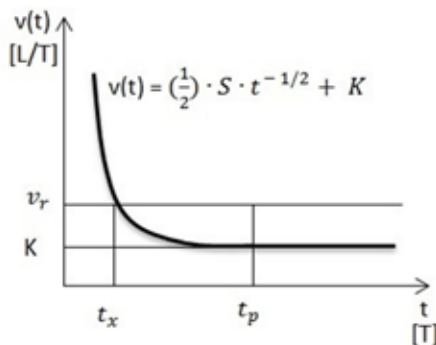


Figure 3. Determination of ponding time t_p from infiltration rate curve and constant rainfall intensity v_r .

Rubin (1966) has shown that the ponding time t_p decreases with an increase of v_r and that $t_p > t_x$, where t_x is the intersection of v_r and the curve $v(t)$, that means $v_r = v(t_x)$, see Equation (9), and t_p is the corresponding time to the K -value of the curve $v(t)$. In order to satisfy boundary conditions as the NBC transforms to DBC, it is assumed that the soil water profiles $W(z, t_p)_N$ and

$W(z, t_x)_D$ are identical. Hence, t_x and t_p must satisfy two conditions (Kutílek and Nielsen, 1994). The first one is Equation (8):

$$t_p \cdot v_r = \int_0^{t_x} v(t) dt \tag{8}$$

The second condition is Equation (9):

$$v_r = v(t_x) \tag{9}$$

Mls (1980) transformed Equations (8) and (9). When Equation (8) is integrated and substituted into Equation (9) and when t_p is expressed, the final expression for ponding time t_p calculation is as follows (Eq. 10):

$$t_p = \left[S \cdot \frac{S}{2(v_r - K)} + K \frac{S^2}{4(v_r - K)^2} \right] / v_r \tag{10}$$

This expression is valid under the hypothesis of a constant rainfall intensity v_r .

Hence, the sorptivity S can be obtained from equation (10) as it follows:

$$S = \frac{\sqrt{2t_p \cdot v_r (v_r - K)}}{\sqrt{1 + \frac{K}{2(v_r - K)}}} \tag{11}$$

This value of S is the most reliable one, as it refers to the pre-saturation condition because it is an estimate of the real sorptivity of the soil before the rainfall event.

Methodology

The single ring infiltrometer method

Determination of hydraulic conductivity of soil surface with a permanent thin water layer, carried out by experimental field measurements and testing with the use of the single ring infiltrometer method was described by Stibinger (2014). Remembering Philip's equation (Eq. 2), under constant rainfall intensity, K can be expressed using the equation (6), once the soil in the infiltrometer ring is fully saturated and sorptivity S goes almost to zero.

In this experiment, a prototype of a single-ring continuous infiltrometer equipped with a rainfall simulator was used. This device enables both to simulate rainfall of various characteristics (intensity, duration, constant or variable intensity) and to measure infiltration rate. A simplified scheme of the device is shown in Fig. 4.

The methodology to calculate ponding time t_p , K and S using a "single ring continuous infiltrometer".

The input parameters used in the experiments were as follows:

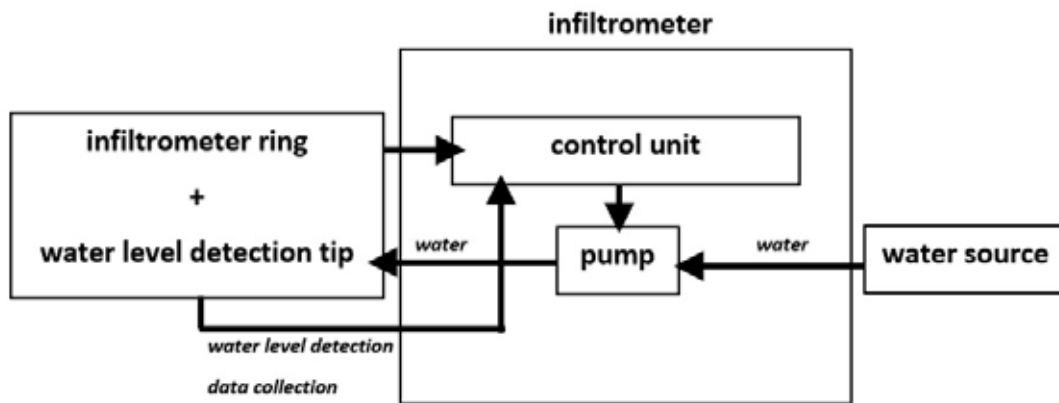


Figure 4. A simplified scheme of a single ring continuous infiltrometer designed for a research project TH02010802

- Infiltrator ring diameter: 100 mm;
- Infiltrator height: 500 mm;
- Simulated rainfall duration time: 15 min;
- Simulated rainfall intensity: 3.0 mm/min (constant during all rainfall event);
- Rainfall depth (total amount): 45.0 mm;
- Ponding level: 5 mm over the soil surface;
- Experiment duration time: 60 min.

The *Central Unit* (Fig. 4) starts to simulate the rainfall in the infiltrator area by the sprinkler. Once the water level reaches the ponding level (5 mm over the average of soil surface – detected by a *water level detection tip*), the ponding time t_p is reached (recorded automatically). Theoretically, the ponding level should be 0 mm above the soil surface. Nevertheless, the water level detection tip is placed a little higher to eliminate errors caused by surface microtopography. A correction is included to deal with this issue during data processing. The *Central Unit* records the values of the time and relative water volume released. A specific software called “*Infiltr View*” (designed in the research project TH02010208) makes the data possible to be converted and used for further analyses in Microsoft Excel. Once the ponding level is reached, W_{t_p} is a water volume considered to be all infiltrated. From this moment on, every next drop

of rainfall will become surface runoff. The rainfall simulation stops at this moment. The next recorded value of water volume released by the device is 0.

Next, the infiltration process continues until contact is lost between the water detection tip and the water layer surface. Once the contact is lost, the rainfall simulation starts again. Input water volume data is recorded (cumulative). New rainfall volume is produced until the ponding level is reached. In this way, the process is repeated until the end of the experiment ($t = 60$ min). The infiltration $i(t)$ of the accumulated water above the surface is measured over time, always referred to the initial values W_{t_p} and t_p . Table 1 provides an example of data processing using the “*Infiltr View*” software.

The infiltration time t and the amount of infiltration $i(t)$ are required when using Philip's infiltration equation (Eq. 2). Infiltration time t is provided when the time of two events (time of reaching the ponding level and time of losing the contact between the tip and water level) is subtracted (infiltration process step by step). The amount of infiltration is the cumulated infiltrated water volume, considered since the ponding time volume. So, both the infiltration time and infiltrated water volume are referred to the relative initial values t_p and W_{t_p} .

Table 1. Example of infiltration $i(t)$ measurement and data processing; bold values refer to ponding time $t_p = 239.76$ s and water volume at ponding time $W_{t_p} = 96.04$ ml.

Device DATA (from “ <i>Infiltr View</i> ”)		ANALYSIS to obtain K, (S = 0), using Philip's equation	
Time [s]	Volume [ml]	Infiltration time t [s]	Infiltration i(t) [mm]
239.76	96.04		
249.18	0	9.42	0.54
254.24	100.31		
264.98	0	25.22	1.07
269.88	104.44		

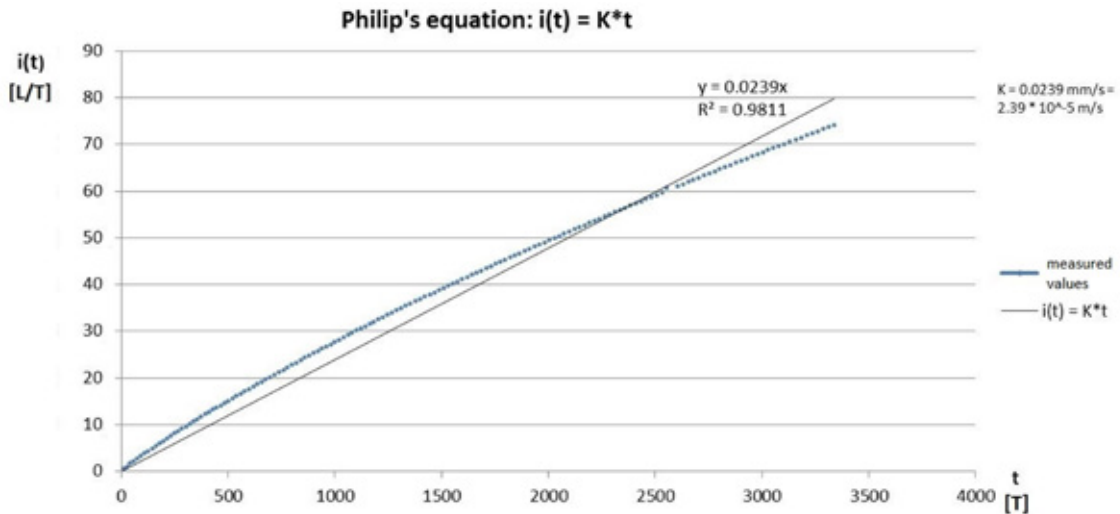


Figure 5. Derivation of K using a graphical expression of Philip's equation)

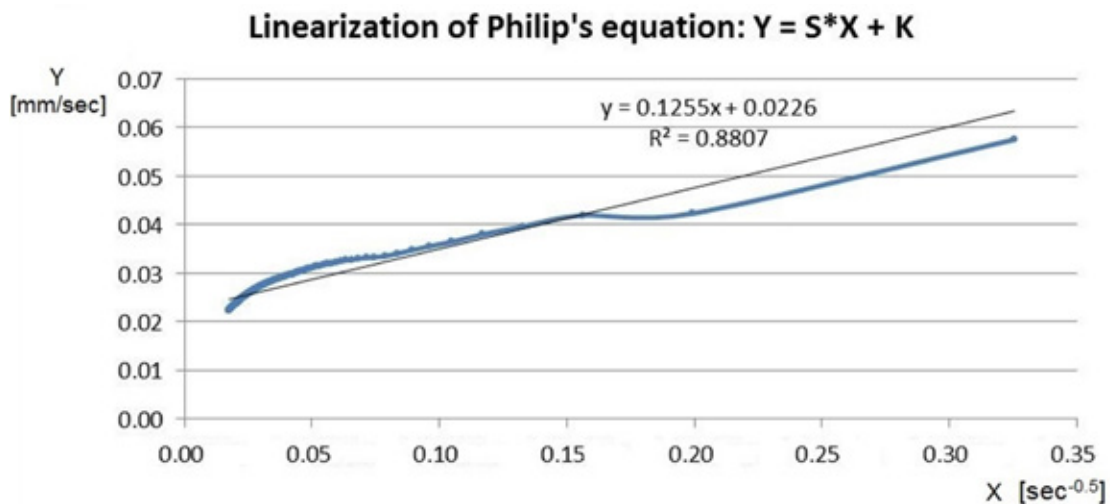


Figure 6. Linearized Philip's equation (Eq. 1) of cumulative infiltration $\left(\frac{1}{\sqrt{t}} = X; \frac{i(t)}{t} = Y\right)$; an illustrative example

Example referring to Table 1:

Infiltration time *t*:

249.18 s – 239.6 s = 9.42 s

264.98 s – 239.6 s = 25.22 s

[...]

Infiltration *i(t)*:

(100.31 ml – 96.04 ml) · 0.127 = 0.54 mm

(104.44 ml – 96.04 ml) · 0.127 = 1.07 mm

[...]

where 0.127 is the conversion coefficient to change millilitres to millimetres.

Since the soil is fully saturated after the ponding time, the sorptivity *S* gets closer to the zero limit, and the expression (Eq. 6) is valid. So, Philip's infiltration curve

can be regarded as a line, and its angular coefficient is the saturated hydraulic conductivity *K* (Fig. 5).

The value of the hydraulic conductivity *K* was approximated as $K = 0.0239 \text{ (mm/sec)} = 2.39 \cdot 10^{-5} \text{ (m/s)} = 0.143 \text{ (cm/min)}$ with correlation coefficient $R = 0.99$ (Fig. 5), which confirms the hypothesis mentioned above and shows that using Philip's linear model was an excellent choice.

Now, there are two different ways to obtain *S*. Either by the linearization of Philip's equation, or by using the rearrangement of Philip's expression of ponding time (Eq. 11).

The linearization of Philip's equation is a method that consists of eliminating the quadratic dependence

in Philip's equation (Eq. 1) by dividing both members by t :

$$i(t) = S \cdot t^{\frac{1}{2}} + K \cdot t \rightarrow \frac{i(t)}{t} = S \cdot \frac{1}{\sqrt{t}} + K \tag{12}$$

$$\frac{i(t)}{t} = Y \tag{13}$$

$$\frac{1}{\sqrt{t}} = X \tag{14}$$

If the variables X and Y from Equations (13) and (14) are used in Equation (12), the final equation (Eq. 15) is derived:

$$Y = S \cdot X + K \tag{15}$$

The Equation (15) represents an equation of a line, where the sorptivity S represents the angular coefficient. By ordering the values of X and Y from the smallest to the highest, the resulting diagram is as follows in Fig. 6.

Linearized Philip's equation (Eq. 2) of cumulative infiltration, see Figure 6, presents **sorptivity $S = 0.125 \text{ (mm/sec}^{0.5}) = 0.097 \text{ (cm/min}^{0.5})$** and hydraulic conductivity $K = 0.0226 \text{ mm/s} = 0.135 \text{ cm/min}$. The high value of correlation coefficient $R = 0.9384$ points at a suitably selected linear regression model.

Nevertheless, the problem with this method is that the S-value is too low since it came out by calculating it experimentally using a saturated soil, where theoretically $S = 0$. Therefore, the better way to get S is by using the Equation (11), obtained from Philip's ponding time equation (Eq. 10).

From the known values of $t_p = \text{approx. } 4 \text{ min}$; $v_r = 0.30 \text{ cm/min}$ and $K = 0.14 \text{ cm/min}$ and with the use of Equation (11) the value of sorptivity $S = 0.51 \text{ cm} \cdot \text{min}^{-1/2}$ can be calculated.

This value of S is the most reliable one, as it refers to the pre-saturation condition (before the rainfall event, when the soil is not completely saturated).

Finally, the value of $K = 0.14 \text{ (cm/min)}$ from linear regression analysis and value of $S = 0.51 \text{ (cm/min}^{0.5})$, found by using Equation (11), were compared with the theoretical values available in literature (Table 2). Table 2 provides values reported by Kutilek and Nielsen (1994).

Comparison of calculated values of K and S and theoretical values form literature

Table 2 provides S values for $K = 0.1$ or 0.2 cm/min . When an interpolation method is used, S referring to $K = 0.14 \text{ (cm/min)}$ should be between the values

Table 2. Theoretical values of K and S depending on soil types (from Kutilek and Nielsen, 1994)

		S [cm/min ^{1/2}]		
K [cm/min]	Sand	Sand/Silt, Silt, Silt/Clay	Clay	
2	2			
1	1.4			
0.9	1.3			
0.8	1.2	2		
0.7	1.1	1.9		
0.6	0.94	1.7		
0.5	0.8	1.5		
0.4	0.65	1.3		
0.3	0.45	1		
0.2	0.28	0.7		
0.1	0.12	0.34		
0.09	0.11	0.31		
0.08	0.1	0.29		
0.07	0.095	0.27		
0.06	0.085	0.24		
0.05	0.075	0.21		
0.04	0.067	0.19		
0.03	0.058	0.17		
0.02	0.05	0.14		
0.01		0.1	0.18	

0.7 cm/min and 0.34 cm/min. This is true for the value of $S = 0.51 \text{ cm} \cdot \text{min}^{-0.5}$.

The authors also considered this method to be applied to the sorptivity S determined from the saturated soil conditions (Figure 6) $S = 0.1255 \text{ mm/min}^{0.5} = 0.1 \text{ cm/min}^{0.5}$. However, in this case, the responding value of K in Table 2 equals to 0.01 cm/min. Nevertheless, this does not correspond to hydro-physical properties of soils types, presented in Table 2. Therefore, sorptivity S before the rainfall event should be considered only. K value can be either calculated from cumulative infiltration curves or determined from the literature.

CONCLUSION

Determination of soil hydraulic properties under non-saturated conditions is crucial to describe soil water dynamics in the field. It is possible to calculate sorptivity from the infiltration data collected after the ponding time, following Philips's theory. However, the sorptivity determined this way tends to reach zero as the soil is fully saturated. Might such a low value of S play any significant role? This paper presents an innovative approach of the soil sorptivity determination, avoiding time-consuming laboratory experiments. A single ring infiltration method, along with a simulation of rainfall of constant intensity, was used to measure ponding

time t_p . Hydraulic conductivity K was approximated from the analysis of time series of the process of vertical non-steady cumulative infiltration appearing after the ponding time. Based on Philip's and Mls's infiltration theory, a simple equation was derived in order to calculate sorptivity S from ponding time t_p , rainfall intensity $i(t)$ and saturated hydraulic conductivity K . Numerically determined results of S correspond closely with theoretical values available in the literature. Such a process of determination of K and S has not been published so far. Unlike the traditional methods, this simple numerical determination provides more precise and representative values of S , verified by ponding time, as they refer to the original (before rainfall event) soil sorptivity – the critical factor for surface runoff formation. This assumption was definitely confirmed by field experimental determination of ponding time and selected soil hydrology characteristics.

ACKNOWLEDGEMENT

This research was funded by the Technology Agency of the Czech Republic, grant TH02010802.

DATA AVAILABILITY STATEMENT

Some or all data, models, or code that support the findings of this study are available from the corresponding author upon reasonable request.

CONFLICT OF INTEREST

The authors declared no conflicts of interest with respect to research, authorship and publication of this article.

ETHICAL COMPLIANCE

The authors have followed the ethical standards in conducting the research and preparing the manuscript.

REFERENCES

- Alfieri L., Salamon P., Pappenberger F., Wetterhall F., Thielen J. (2012): Operational early warning systems for water-related hazards in Europe. *Environmental Science Policy* 21: 35–49.
- Angulo-Jaramillo R., Vandervaere J. P., Roulier S., Thony J. L., Gaudet J. P., Vauclin M. (2000): Field measurement of soil surface hydraulic properties by disc and ring infiltrometers: A review and recent developments. *Soil & Tillage Research* 55: 1–29.
- Borga M., Anagnostou E. N., Blöschl G., Creutin J. D. (2011): Flash flood forecasting, warning and risk management: the HYDRATE project. *Environmental Science Policy* 14: 834–844.
- Carpenter T. M., Sperflage J. A., Georgakakos K. P., Sweeney T., Fread D. L. (1999): National threshold runoff estimation utilizing GIS in support of operational flash flood warning systems. *Journal of Hydrology* 224: 21–44.
- Dirmeyer P. A., Cash B. A., Kinter III J. L., Stan C., Jung T., Marx, L., Huang, B. (2012): Evidence for enhanced land-atmosphere feedback in a warming climate. *Journal of Hydrometeorology* 13: 981–995.
- Fuentes C., Zavala M., Saucedo H. (2009): Relationship between the Storage Coefficient and the Soil-Water Retention Curve in Subsurface Agricultural Drainage Systems: Water Table Drawdown. *Journal of Irrigation and Drainage Engineering* 135: 279–285.
- Georgakakos K. P. (2006): Analytical results for operational flash flood guidance. *Journal of Hydrology* 317: 81–103.
- Hanks R. J., Ashcroft G. L. (1976): Physical properties of soils. Department of Soil Science and Meteorology. Utah State University.
- Hapuarachchi H. A. P., Wang Q. J., Pagano T. C. (2011): A review of advances in flash flood forecasting. *Hydrological Processes* 25: 2771–2784.
- Javelle P., Fouchier C., Arnaud P., Lavabre J. (2010): Flash flood warning at ungauged locations using radar rainfall and antecedent soil moisture estimations. *Journal of Hydrology* 394: 267–274.
- Jaynes R. A., Gifford G. F. (1981): An in-depth examination of the Philip equation for cataloging infiltration characteristics in rangeland environments. *RE & M* 34: 285–296.
- Kutílek M., Nielsen D. R. (1994): Soil hydrology: textbook for students of soil science, agriculture, forestry, geoecology, hydrology, geomorphology and other related disciplines. Catena Verlag.
- Menzel L., Kundzewicz Z. W. (2003): Non-Structural Flood Protection-A Challenge. International Conference Towards National Flood Reduction Strategies. Water International Warsaw 6–13: 223–248.
- Mirlas V. (2009): Applying MODFLOW Model for Drainage Problem Solution: A Case Study from Jahir Irrigated Fields. Israel. *Journal of Irrigation and Drainage Engineering* 135: 269–278.
- Mls J. (1980): Effective rainfall estimation. *Journal of Hydrology* 45: 305–311.
- Norbiato D., Borga M., Degli Esposti S., Gaume E., Anquetin S. (2008): Flash flood warning based on rainfall thresholds and soil moisture conditions: An assessment for gauged and ungauged basins. *Journal of Hydrology* 362: 274–290.

- Ntelekos A. A., Georgakakos K. P., Krajewski W. F. (2006): On the uncertainties of flash flood guidance: Toward probabilistic forecasting of flash floods. *Journal of Hydrometeorology* 75: 896–915.
- Philip J. R. (1957a): Numerical solutions of equations of the diffusion type with diffusivity concentration dependent. II. *Australian Journal of Physics* 10: 29–42.
- Philip J. R. (1957b): The theory of infiltration: 1. The infiltration equation and its solution. *Soil Science* 83: 345–357.
- Polger P. D., Goldsmith B. S., Przywarty R. C., Bocchieri J. R. (1994): National Weather Service warning performance based on the WSR-88D.B. *American Meteorological Society* 75: 203–214.
- Rubin J. (1966): Theory of rainfall uptake by soils initially drier than their field capacity and its applications. *Water Resources* 24: 739–749.
- Singh S. K. (2009): Generalized analytical Solutions for Groundwater Head in a horizontal Aquifer in the Presence of Subsurface Drains. *Journal of Irrigation and Drainage Engineering* 135: 295–302.
- Stibinger J. (2014): Drainage Retention Capacity (DREC) of Krisak Mountain Meadows Agricultural Area (Jizera Mountains, Czech Republic) for Mitigation of Negative Impacts of Climate Change. <http://www.elsevier.com/electronic-products/procedia> (April 25, 2016).
- Villarreal R., Lozano L. A., Melani E. M., Salazar M. P., Otero M. F., Soracco C. G. (2019): Diffusivity and sorptivity determination at different soil water contents from horizontal infiltration. *Geoderma* 338: 88–96.
- Whitehead P. G., Wilby R. L., Battarbee R. W., Kernan M., Wade A. J. (2009): A review of the potential impacts of climate change on surface water quality. *Hydrological Science Journal* 54: 101–123.
- Zhang R. (1997). Determination of soil sorptivity and hydraulic conductivity from the disk infiltrometer. *Soil Science Society American Journal* 6: 1024–1030.

Received February 8, 2023

Accepted after revisions: March 30, 2023